

# Engineering Notes

## Asymptotic Analysis of Displaced Lunar Orbits

Jules Simo\* and Colin R. McInnes†

University of Strathclyde,

Glasgow, Scotland G1 1XJ, United Kingdom

DOI: 10.2514/1.43703

### Introduction

THE design of spacecraft trajectories is a crucial task in space mission design. Solar sail technology appears as a promising form of advanced spacecraft propulsion which can enable exciting new space-science mission concepts such as solar system exploration and deep space observation. Although solar sailing has been considered as a practical means of spacecraft propulsion only relatively recently, the fundamental ideas are by no means new (see McInnes [1] for a detailed description). A solar sail is propelled by reflecting solar photons and therefore can transform the momentum of the photons into a propulsive force. Solar sails can also be utilized for highly non-Keplerian orbits, such as orbits displaced high above the ecliptic plane (see Waters and McInnes [2]). Solar sails are especially suited for such non-Keplerian orbits, because they can apply a propulsive force continuously. In such trajectories, a sail can be used as a communication satellite for high latitudes. For example, the orbital plane of the sail can be displaced above the orbital plane of the Earth, so that the sail can stay fixed above the Earth at some distance, if the orbital periods are equal (see Forward [3]). Orbit around the collinear points of the Earth–moon system are also of great interest because their unique positions are advantageous for several important applications in space mission design (see, e.g., Szebehely [4], Roy [5], Vonbun [6], Thurman and Worfolk [7], Gómez et al. [8,9]). Several authors have tried to determine more accurate approximations (quasi-halo orbits) of such equilibrium orbits [10]. These orbits were first studied by Farquhar [11], Farquhar and Kamel [10], Breakwell and Brown [12], Richardson [13], Howell [14], and Howell and Marchand [15]. If an orbit maintains visibility from Earth, a spacecraft on it (near the  $L_2$  point) can be used to provide communication between the equatorial regions of the Earth and the lunar poles. The establishment of a bridge for radio communications is crucial for forthcoming space missions, which plan to use the lunar poles. McInnes [16] investigated a new family of displaced solar sail orbits near the Earth–moon libration points. Displaced orbits have more recently been developed by Ozimek et al. [17] using collocation methods. In Baoyin and McInnes [18–20] and McInnes [16,21], the authors describe new orbits which are associated with artificial Lagrange points in the Earth–sun system. These artificial equilibria have potential applications for future space physics and Earth observation missions. In McInnes et al. [22], the

authors investigate large new families of solar sail orbits, such as sun-centered halo-type trajectories, with the sail executing a circular orbit of a chosen period above the ecliptic plane. We have recently investigated displaced periodic orbits at linear order in the Earth–moon restricted three-body system, where the third massless body is a solar sail (see Simo and McInnes [23]). These highly non-Keplerian orbits are achieved using an extremely small sail acceleration. It was found that for a given displacement distance above/below the Earth–moon plane it is easier by a factor of order 3.19 to do so at  $L_4/L_5$  compared to  $L_1/L_2$ , that is, for a fixed sail acceleration the displacement distance at  $L_4/L_5$  is greater than that at  $L_1/L_2$ . In addition, displaced  $L_4/L_5$  orbits are passively stable, making them more forgiving to sail pointing errors than highly unstable orbits at  $L_1/L_2$ . The drawback of the new family of orbits is the increased telecommunications path length, particularly the moon– $L_4$  distance compared to the moon– $L_2$  distance.

In this Note, we study the dynamics of displaced orbits in relation to the two- and three-body Earth–moon problem and compare the results. The solar sail Earth–moon problem differs greatly from the Earth–sun system as the sun-line direction varies continuously in the rotating frame and the equations of motion of the sail are given by a set of nonlinear, nonautonomous ordinary differential equations. Trajectories near the Earth–moon  $L_1$  and  $L_2$  points are not easily identified, such that the solar sail can enable continuous communication with the equatorial regions of the Earth from any point on the lunar far side. We therefore develop an asymptotic analysis for large ( $a_0 = 1.7 \text{ mm/s}^2$ ) and small ( $a_0 = 0.58 \text{ mm/s}^2$ ) accelerations. This analysis is obtained within an approximation of large displaced orbits ( $a_0 = 1.7 \text{ mm/s}^2$ ) by the moon–sail two-body problem. The displaced periodic orbits found approach the asymptotic solutions as the characteristic acceleration becomes large. It is shown, for example, that, with a suitable sail attitude control program, a  $4 \times 10^4 \text{ km}$  displaced, out-of-plane trajectory far from the  $L_2$  with a sail acceleration of  $1.7 \text{ mm s}^{-2}$  can be approximated using the two-body analysis. This simple, two-body approximate analysis matches with the large displaced orbit found by Ozimek et al. [17] using numerical collocation methods in a previous study. For small acceleration we use a linear approximation of the Earth–moon three-body problem which again matches well with Ozimek et al. [17].

### Moon–Sail Three-Body Problem

The motion of a solar sail moving under the gravitational influences of the Earth and the moon can be described in terms of the circular restricted three-body problem. In this model, we will assume that  $m_1$  represents the larger primary (Earth),  $m_2$  the smaller primary (moon), and we will be concerned with the motion of the sail which has a negligible mass ( $m_1 > m_2$ ). It is always assumed that the two more massive bodies (primaries) move in circular orbits about their common center of mass. If we further restrict the motion of the third body to be in the orbital plane formed by the other two bodies, the problem is the planar circular restricted three-body problem. To develop a mathematical model without loss of generality, it is useful to introduce some parameters that are characteristics of each particular three-body system. This set of parameters is used to normalize the equations of motion. The unit of mass is taken to be the total mass of the system ( $m_1 + m_2$ ) and the unit of length is chosen to be the constant separation between  $m_1$  and  $m_2$ . We further define the time units such that, the orbital period of the primaries about their center of mass is  $2\pi$ . Under these considerations the masses of the primaries in the normalized system of units are  $m_1 = 1 - \mu$  and  $m_2 = \mu$ , where

$$\mu = \frac{m_2}{m_1 + m_2} \quad (1)$$

Received 7 February 2009; revision received 2 June 2009; accepted for publication 2 June 2009. Copyright © 2009 by the American Institute of Aeronautics and Astronautics, Inc. All rights reserved. Copies of this paper may be made for personal or internal use, on condition that the copier pay the \$10.00 per-copy fee to the Copyright Clearance Center, Inc., 222 Rosewood Drive, Danvers, MA 01923; include the code 0731-5090/09 and \$10.00 in correspondence with the CCC.

\*Research Fellow, Department of Mechanical Engineering, James Weir Building, 75 Montrose Street; jules.simo@strath.ac.uk.

†Professor, Department of Mechanical Engineering, James Weir Building, 75 Montrose Street; colin.mcinnes@strath.ac.uk. Member AIAA

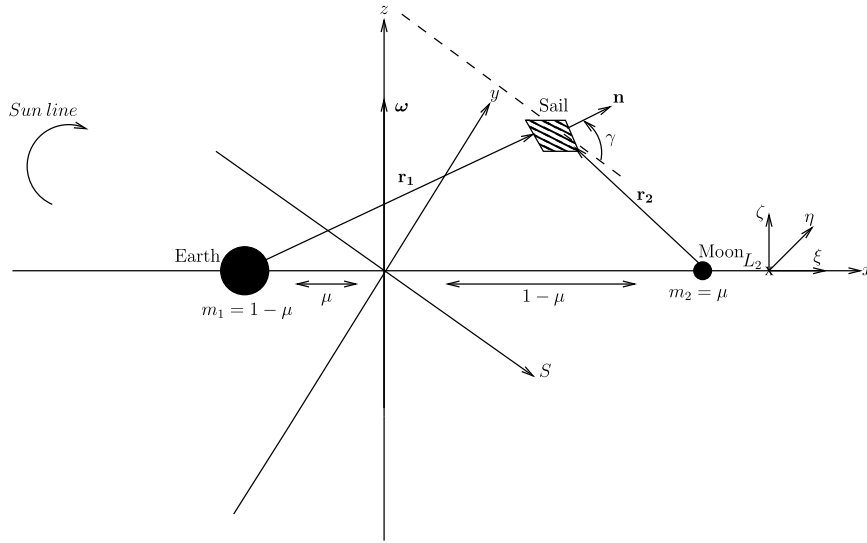


Fig. 1 Schematic geometry of the Earth–moon restricted three-body problem.

is the nondimensional gravitational parameter. The geometry for the Earth–moon restricted three-body system is depicted in Fig. 1.

#### Equations of Motion in Presence of a Solar Sail

The equation for the solar sail in a rotating frame of reference is described by

$$\frac{d^2\mathbf{r}}{dt^2} + 2\boldsymbol{\omega} \times \frac{d\mathbf{r}}{dt} + \nabla U(\mathbf{r}) = \mathbf{a} \quad (2)$$

where  $\boldsymbol{\omega} = \omega \hat{\mathbf{z}}$  ( $\hat{\mathbf{z}}$  is a unit vector pointing in the direction of  $\mathbf{z}$ ) is the angular velocity vector of the rotating frame and  $\mathbf{r}$  is the position vector of the solar sail relative to the center of mass of the two primaries. The three-body gravitational potential  $U(\mathbf{r})$  and the solar radiation pressure acceleration  $\mathbf{a}$  are defined by

$$U(\mathbf{r}) = -\left[\frac{1}{2}|\boldsymbol{\omega} \times \mathbf{r}|^2 + \frac{1-\mu}{r_1} + \frac{\mu}{r_2}\right], \quad \mathbf{a} = a_0(\mathbf{S} \cdot \mathbf{n})^2 \mathbf{n} \quad (3)$$

where  $\mu = 0.1215$  is the mass ratio for the Earth–moon system. The sail position vectors with respect to  $m_1$  and  $m_2$ , respectively, are defined as  $\mathbf{r}_1 = [x + \mu, y, z]^T$  and  $\mathbf{r}_2 = [x - (1 - \mu), y, z]^T$ , and  $a_0$  is the magnitude of the acceleration due to solar radiation pressure exerted on the sail. The unit normal to the sail  $\mathbf{n}$  and the sun-line direction are given by

$$\begin{aligned} \mathbf{n} &= [\cos(\gamma) \cos(\omega_* t) \quad -\cos(\gamma) \sin(\omega_* t) \quad \sin(\gamma)]^T \\ \mathbf{S} &= [\cos(\omega_* t) \quad -\sin(\omega_* t) \quad 0]^T \end{aligned}$$

where  $\omega_* = 0.923$  is the angular rate of the sun line in the corotating frame in a dimensionless synodic coordinate system. We will not consider the small annual changes in the inclination of the sun line with respect to the plane of the system.

#### Linearized System

We now investigate the dynamics of the sail in the neighborhood of the libration points. We denote the coordinates of the equilibrium point as  $\mathbf{r}_L = (x_{L_i}, y_{L_i}, z_{L_i})$  with  $i = 1, \dots, 5$ . Let a small displacement in  $\mathbf{r}_L$  be  $\delta\mathbf{r}$  such that  $\mathbf{r} \rightarrow \mathbf{r}_L + \delta\mathbf{r}$ . The equations of motion for the solar sail in the neighborhood of  $\mathbf{r}_L$  are therefore

$$\frac{d^2\delta\mathbf{r}}{dt^2} + 2\boldsymbol{\omega} \times \frac{d\delta\mathbf{r}}{dt} + \nabla U(\mathbf{r}_L + \delta\mathbf{r}) = \mathbf{a}(\mathbf{r}_L + \delta\mathbf{r}) \quad (4)$$

Then, retaining only the first-order term in  $\delta\mathbf{r} = [\xi, \eta, \zeta]^T$  in a Taylor-series expansion, where  $(\xi, \eta, \zeta)$  are attached to the  $L_2$  point as shown in Fig. 1, the gradient of the potential and the acceleration can be expressed as

$$\nabla U(\mathbf{r}_L + \delta\mathbf{r}) = \nabla U(\mathbf{r}_L) + \left. \frac{\partial \nabla U(\mathbf{r})}{\partial \mathbf{r}} \right|_{\mathbf{r}=\mathbf{r}_L} \delta\mathbf{r} + O(\delta\mathbf{r}^2) \quad (5)$$

$$\mathbf{a}(\mathbf{r}_L + \delta\mathbf{r}) = \mathbf{a}(\mathbf{r}_L) + \left. \frac{\partial \mathbf{a}(\mathbf{r})}{\partial \mathbf{r}} \right|_{\mathbf{r}=\mathbf{r}_L} \delta\mathbf{r} + O(\delta\mathbf{r}^2) \quad (6)$$

It is assumed that  $\nabla U(\mathbf{r}_L) = 0$ , and the sail acceleration is constant with respect to the small displacement  $\delta\mathbf{r}$ , so that

$$\left. \frac{\partial \mathbf{a}(\mathbf{r})}{\partial \mathbf{r}} \right|_{\mathbf{r}=\mathbf{r}_L} = 0 \quad (7)$$

The linear variational system associated with the libration points at  $\mathbf{r}_L$  can be determined through a Taylor polynomial by substituting Eqs. (6) and (7) into Eq. (4)

$$\frac{d^2\delta\mathbf{r}}{dt^2} + 2\boldsymbol{\omega} \times \frac{d\delta\mathbf{r}}{dt} - K\delta\mathbf{r} = \mathbf{a}(\mathbf{r}_L) \quad (8)$$

where the matrix  $K$  is defined as

$$K = -\left[ \left. \frac{\partial \nabla U(\mathbf{r})}{\partial \mathbf{r}} \right|_{\mathbf{r}=\mathbf{r}_L} \right] \quad (9)$$

Using the matrix notation the linearized equation about the libration point [Eq. (8)] can be represented by the inhomogeneous linear system  $\dot{\mathbf{X}} = \mathbf{A}\mathbf{X} + \mathbf{b}(t)$ , where the state vector  $\mathbf{X} = (\delta\mathbf{r}, \dot{\delta\mathbf{r}})^T$ , and  $\mathbf{b}(t)$  is a  $6 \times 1$  vector, which represents the solar sail acceleration.

The Jacobian matrix  $\mathbf{A}$  has the general form

$$\mathbf{A} = \begin{pmatrix} 0_3 & I_3 \\ K & \Omega \end{pmatrix} \quad (10)$$

where  $I_3$  is a identity matrix, and

$$\Omega = \begin{pmatrix} 0 & 2 & 0 \\ -2 & 0 & 0 \\ 0 & 0 & 0 \end{pmatrix} \quad (11)$$

For convenience the sail attitude is fixed such that the sail normal vector  $\mathbf{n}$  points always along the direction of the sun line with the following constraint  $\mathbf{S} \cdot \mathbf{n} \geq 0$ . Its direction is described by the pitch angle  $\gamma$  relative to the sun line, which represents the sail attitude. The linearized nondimensional equations of motion relative to a collinear libration point  $L_2$  can then be written as

$$\ddot{\xi} - 2\dot{\eta} - U_{xx}^o \xi = a_\xi \quad (12)$$

$$\ddot{\eta} + 2\dot{\xi} - U_{yy}^o \eta = a_\eta \quad (13)$$

$$\ddot{\zeta} - U_{zz}^o \zeta = a_\zeta \quad (14)$$

where  $U_{xx}^o$ ,  $U_{yy}^o$ , and  $U_{zz}^o$  are the partial derivatives of the gravitational potential evaluated at the collinear libration point, and the solar sail acceleration is defined in terms of three auxiliary variables  $a_\xi$ ,  $a_\eta$ , and  $a_\zeta$

$$a_\xi = a_0 \cos(\omega_* t) \cos^3(\gamma) \quad (15)$$

$$a_\eta = -a_0 \sin(\omega_* t) \cos^3(\gamma) \quad (16)$$

$$a_\zeta = a_0 \cos^2(\gamma) \sin(\gamma) \quad (17)$$

We will continue with the solution to the linearized equations of motion in the Earth–moon restricted three-body problem in a later section.

### Moon–Sail Two-Body Problem

In this section, we consider the motion of a solar sail moving under the gravitational influence of the moon only as shown in Fig. 2. Such a problem is defined as the moon–sail two-body problem. For a large displacement, such that the sail is far from the  $L_1$  or  $L_2$  point, this provides a remarkably good approximation to the problem. The forces acting on the sail can be seen in Fig. 3.

In this model, the moon is assumed to be fixed, while the solar sail is in a rotating frame of reference. To describe the motion of the sail, we take a reference frame rotating with the sun line at angular velocity  $\omega_*$ , such that the origin is at the center  $c$ . We write the two-body equations in a similar form to Eq. (2). In the rotating frame  $\ddot{\mathbf{r}} = \dot{\mathbf{r}} = 0$  and we have the equality

$$\nabla \tilde{U}(\mathbf{r}) = \mathbf{a} \quad (18)$$

where

$$\tilde{U}(\mathbf{r}) = -\left[\frac{1}{2}|\boldsymbol{\omega}_* \times \mathbf{r}|^2 + \frac{Gm_2}{r}\right] \quad (19)$$

The equations of motion of the solar sail in component form may be written in cylindrical coordinates  $(\rho, z)$  as

$$\frac{Gm_2}{r^2} \cos(\theta) = a_0 \cos^2(\gamma) \sin(\gamma) \quad (20)$$

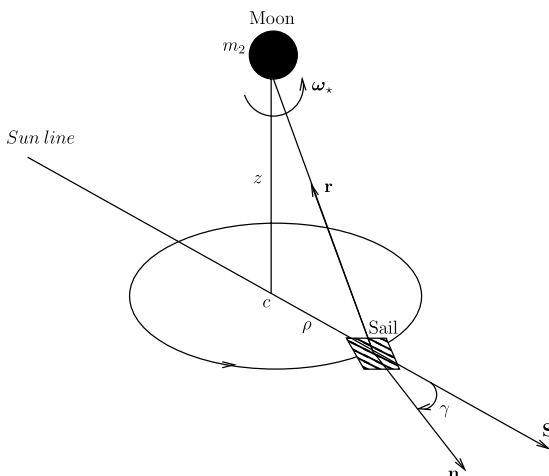


Fig. 2 Schematic geometry of the moon–sail two-body problem generating a hover orbit.

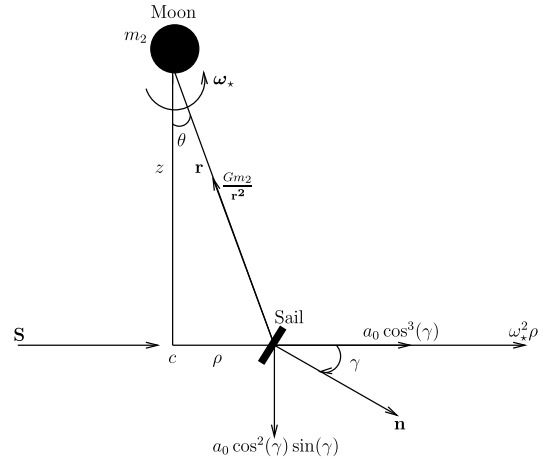


Fig. 3 Representative forces.

$$\frac{Gm_2}{r^2} \sin(\theta) - \omega_*^2 \rho = a_0 \cos^3(\gamma) \quad (21)$$

with  $\cos(\theta) = \frac{z}{r}$ ,  $\sin(\theta) = \frac{\rho}{r}$ , where  $m_2$  is the mass of the moon,  $G$  is the gravitational constant, and the distance of the solar sail from the moon is  $r = \sqrt{\rho^2 + z^2}$  so that

$$\frac{Gm_2 z}{r^3} = a_0 \cos^2(\gamma) \sin(\gamma) \quad (22)$$

$$\frac{Gm_2 \rho}{r^3} = a_0 \cos^3(\gamma) + \omega_*^2 \rho \quad (23)$$

Rearranging Eqs. (22) and (23), we obtain

$$\tan(\gamma) = \frac{z}{\rho} \left[ 1 - \left( \frac{\omega_*}{\tilde{\omega}} \right)^2 \right]^{-1} \quad (24)$$

for a given  $(\rho, z)$ , where

$$\tilde{\omega}^2 = \frac{Gm_2}{r^3} \quad (25)$$

Similary from Eqs. (22) and (23), the required radiation pressure acceleration for the two-body analysis may also be obtained as

$$a_0 = \cos^2(\gamma)^{-1} [(\tilde{\omega}^2 z)^2 + (\tilde{\omega}^2 \rho - \omega_*^2 \rho)^2]^{1/2} \quad (26)$$

We now have conditions for a large displaced periodic orbit centered on the moon. We will evaluate the usefulness of this model later.

### Solution of the Linearized Equations of Motion for the Three-Body Model

To evaluate the two- and three-body models, we will obtain a displaced periodic orbit from the linearized dynamics defined earlier.

Considering the dynamics of motion near the collinear libration points, we may choose a particular periodic solution in the plane of the form (see Farquhar [24])

$$\xi(t) = \xi_0 \cos(\omega_* t) \quad (27)$$

$$\eta(t) = \eta_0 \sin(\omega_* t) \quad (28)$$

By inserting Eqs. (27) and (28) in the differential equations (12–14), we obtain the linear system in  $\xi_0$  and  $\eta_0$ ,

$$\begin{aligned} (U_{xx}^o - \omega_*^2) \xi_0 - 2\omega_* \eta_0 &= a_0 \cos^3(\gamma), \\ -2\omega_* \xi_0 + (U_{yy}^o - \omega_*^2) \eta_0 &= -a_0 \cos^3(\gamma) \end{aligned} \quad (29)$$

Then the amplitudes  $\xi_0$  and  $\eta_0$  are given by

$$\xi_0 = a_0 \frac{(U_{yy}^o - \omega_*^2 - 2\omega_* \cos^3(\gamma))}{(U_{xx}^o - \omega_*^2)(U_{yy}^o - \omega_*^2) - 4\omega_*^2} \quad (30)$$

$$\eta_0 = a_0 \frac{(-U_{xx}^o + \omega_*^2 + 2\omega_* \cos^3(\gamma))}{(U_{xx}^o - \omega_*^2)(U_{yy}^o - \omega_*^2) - 4\omega_*^2} \quad (31)$$

and we have the equality

$$\frac{\xi_0}{\eta_0} = \frac{\omega_*^2 + 2\omega_* - U_{yy}^o}{-\omega_*^2 - 2\omega_* + U_{xx}^o} \quad (32)$$

The trajectory will therefore be an ellipse centered on a collinear libration point. We can find the required radiation pressure acceleration by solving Eq. (30)

$$a_0 = \cos^{-3}(\gamma) \left[ \frac{\omega_*^4 - \omega_*^2(U_{xx}^o + U_{yy}^o + 4) + U_{xx}^o U_{yy}^o}{U_{yy}^o - 2\omega_* - \omega_*^2} \right] \xi_0$$

By applying the Laplace transform, the uncoupled out-of-plane  $\zeta$  motion defined by Eq. (14) can be obtained as

$$\begin{aligned} \zeta(t) = & U(t) a_0 \cos^2(\gamma) \sin(\gamma) |U_{zz}^o|^{-1} + \dot{\zeta}_0 |U_{zz}^o|^{-1/2} \sin(\omega_\zeta t) \\ & + \cos(\omega_\zeta t) [\zeta_0 - a_0 \cos^2(\gamma) \sin(\gamma) |U_{zz}^o|^{-1}] \end{aligned} \quad (33)$$

where the nondimensional frequency  $\omega_\zeta$  is defined as

$$\omega_\zeta = |U_{zz}^o|^{1/2}$$

and  $U(t)$  is the unit step function.

A sufficient condition for displaced orbits based on the sail pitch angle  $\gamma$  and the magnitude of the solar radiation pressure  $a_0$  for fixed initial out-of-plane distance  $\zeta_0$  can be derived. Specifically for the choice of the initial data  $\dot{\zeta}_0 = 0$ , Eq. (33) can be more conveniently expressed as

$$\begin{aligned} \zeta(t) = & U(t) a_0 \cos^2(\gamma) \sin(\gamma) |U_{zz}^o|^{-1} \\ & + \cos(\omega_\zeta t) [\zeta_0 - a_0 \cos^2(\gamma) \sin(\gamma) |U_{zz}^o|^{-1}] \end{aligned} \quad (34)$$

The solution can then be made to contain only a constant displacement at an out-of-plane distance

$$\zeta_0 = a_0 \cos^2(\gamma) \sin(\gamma) |U_{zz}^o|^{-1} \quad (35)$$

Furthermore, the out-of-plane distance can be maximized by an optimal choice of the sail pitch angle determined by

$$\frac{d}{d\gamma^*} \cos^2(\gamma^*) \sin(\gamma^*) = 0 \quad (36)$$

$$\gamma^* = 35^\circ.264 \quad (37)$$

We now have conditions for a small displaced periodic orbit centered on the collinear libration points.

### Comparison of the Linear Three-Body and the Approximate Two-Body Solution

In this section, we compare the dynamics near the Earth-Moon  $L_1$  and  $L_2$  points for small accelerations with the linear analysis, and the large hover orbits for large acceleration with the two-body analysis to the orbit found by Ozimek et al. [17] using a full three-body analysis. We demonstrate that for a given orbit radius  $\rho$  and displacement distance  $z$ , we can find the characteristic acceleration  $a_0$  and the sail pitch angle  $\gamma$  using the two-body analysis.

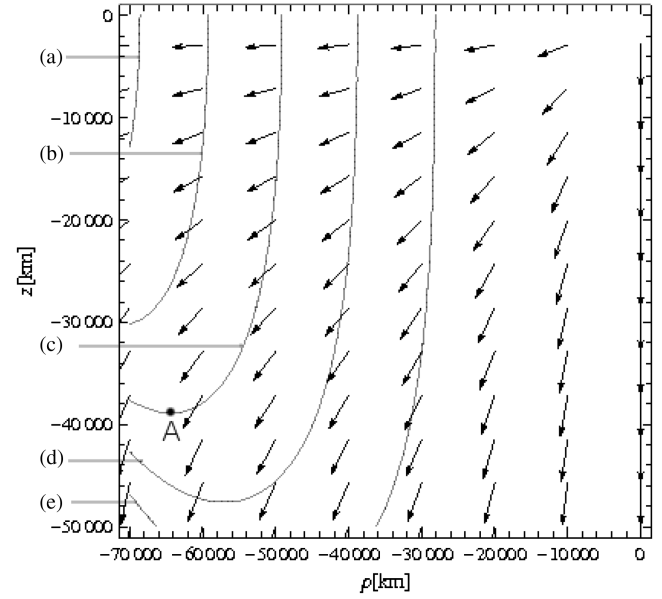


Fig. 4 A contour plot and the vector field of the characteristic acceleration  $a_0 = a_0(\rho, z)$  in the Earth-moon system: a)  $a_0 = 0.58 \text{ mm/s}^2$ , b)  $a_0 = 1 \text{ mm/s}^2$ , c)  $a_0 = 1.7 \text{ mm/s}^2$ , d)  $a_0 = 3 \text{ mm/s}^2$ , and e)  $a_0 = 6 \text{ mm/s}^2$ .

Let us consider the vector field on the plane given by

$$\mathbf{n}(\rho, z) = \left( \frac{f_2(\rho, z)}{\sqrt{f_1^2(\rho, z) + f_2^2(\rho, z)}}, \frac{f_1(\rho, z)}{\sqrt{f_1^2(\rho, z) + f_2^2(\rho, z)}} \right) \quad (38)$$

where

$$f_1(\rho, z) = \frac{Gm_2 z}{r^3} \quad (39)$$

$$f_2(\rho, z) = \frac{Gm_2 \rho}{r^3} - \omega^2 \rho \quad (40)$$

For a given  $(\rho, z)$  the contours of Fig. 4 define the require sail acceleration  $a_0$  from Eq. (26) while the vector field describes the

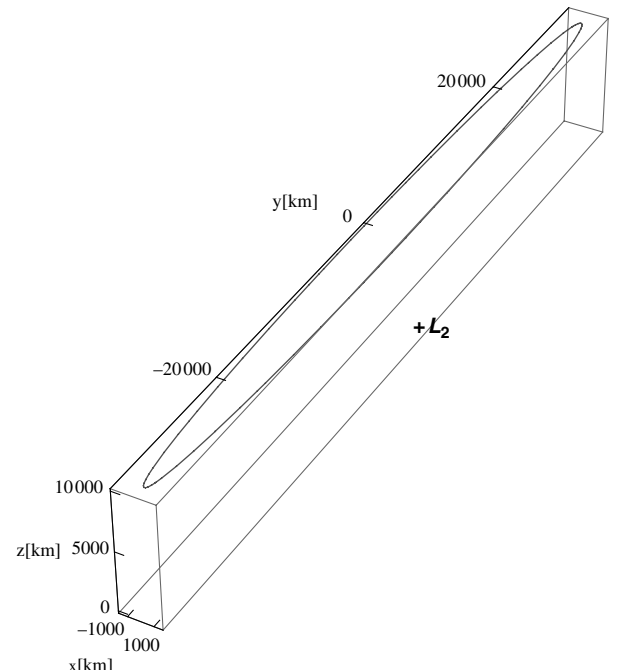


Fig. 5 Linear analysis for small  $a_0 = 0.58 \text{ mm/s}^2$  (orbit around  $L_2$ ).

**Table 1 Comparison of displacement distance and orbit radius**

$a_0$ , mm/s <sup>2</sup>	$z$ , km <sup>a</sup>	$z$ , km <sup>b</sup>	$\rho$ , km <sup>a</sup>	$\rho$ , km <sup>b</sup>
0.58	$\approx 10^4$	$\approx 10^4$ <sup>c</sup>	—	—
1.70	$\approx 4.5 \times 10^4$	$\approx 4.0 \times 10^4$ <sup>d</sup>	$\approx 5.6 \times 10^4$	$\approx 6.0 \times 10^4$

<sup>a</sup>Displacement and radius found by Ozimek et al. using Hermite–Simpson and seventh-degree Gauss Lobatto collocation schemes [17].

<sup>b</sup>Displacement and radius found by the approximate analysis in this paper.

<sup>c</sup>Displacement distance obtain from the linear analytical solution.

<sup>d</sup>Displacement distance obtain from the two-body approximation.

required sail orientation  $\mathbf{n}$ . From Eqs. (22) and (23), this vector field defined on the whole plane minus the origin describes the direction of the acceleration vector  $\mathbf{a} = \mathbf{a}(\rho, z)$ .

This figure indicates for a large characteristic acceleration  $a_0 = 1.7$  mm/s<sup>2</sup>, an orbit with radius  $\rho \approx 6 \times 10^4$  km and displacement distance  $z \approx 4 \times 10^4$  km is possible. The point marked A in Fig. 4 represents the optimal displaced orbit. A small orbit at  $L_2$  with characteristic acceleration  $a_0 = 0.58$  mm/s<sup>2</sup> is shown in Fig. 5 using the linear analysis.

Near  $L_1$  and  $L_2$  the displacement distance for the linear analysis for a small acceleration  $a_0 = 0.58$  mm/s<sup>2</sup> and the two-body analysis for large acceleration  $a_0 = 1.7$  mm/s<sup>2</sup> give a good approximation to the orbits found by Ozimek et al. [17] using a full three-body analysis (see Table 1).

## Conclusions

This paper has demonstrated the approximation of large displaced orbits in the Earth–moon circular restricted three-body problem by the moon–sail two-body problem. In addition, based on the linearized equation of motion near the collinear Lagrange points, displaced periodic orbits can be approximated by using linear analytical analysis, whereas far from those points the classical two-body problem gives a good approximation. A sufficient condition for displaced periodic orbits based on the sail pitch angle and the magnitude of the solar radiation pressure for fixed initial out-of-plane distance has been derived. It was shown that for a given orbit radius and displacement distance, we can find the characteristic acceleration and the sail pitch angle using the two-body analysis. The orbits found approach the asymptotic solutions as the characteristic acceleration becomes large. A particular use of such orbits include continuous communications between the equatorial regions of the Earth and the lunar poles.

## Acknowledgment

This work was funded by the European MCRTN (Marie Curie Research Training Network) AstroNet, Contract Grant No. MRTN-CT-2006-035151.

## References

- [1] McInnes, C. R., *Solar Sailing: Technology, Dynamics and Mission Applications*, Springer Praxis, London, 1999, pp. 11–29.
- [2] Waters, T., and McInnes, C., “Periodic Orbits Above the Ecliptic in the Solar-Sail Restricted Three-Body Problem,” *Journal of Guidance, Control, and Dynamics*, Vol. 30, No. 3, 2007, pp. 687–693. doi:10.2514/1.26232
- [3] Forward, R. L., “Statite: A Spacecraft That Does Not Orbit,” *Journal of Spacecraft and Rockets*, Vol. 28, No. 5, 1991, pp. 606–611.

doi:10.2514/3.26287

- [4] Szebehely, V., *Theory of Orbits: The Restricted Problem of Three Bodies*, Academic Press, New York, 1967, pp. 497–525.
- [5] Roy, A. E., *Orbital Motion*, Institute of Physics Publishing, Bristol, 2005, pp. 118–130.
- [6] Vonbun, F., “A Humminbird for the  $L_2$  Lunar Libration Point,” NASA TN-D-4468, April 1968.
- [7] Thurman, R., and Worfolk, P., “The Geometry of Halo Orbits in the Circular Restricted Threebody Problem,” Geometry Center, University of Minnesota, TR GCG95, 1996.
- [8] Gómez, G., Llibre, J., Martnez, R., and Simó, C., *Dynamics and Mission Design Near Libration Points*, World Scientific, Singapore, 2001, Vol. 2, Chaps. 1, 2.
- [9] Gómez, G., Jorba, A., Masdemont, J., and Simó, C., *Dynamics and Mission Design Near Libration Points*, World Scientific, Singapore, 2001, Vol. 4, Chap. 2.
- [10] Farquhar, R., and Kamel, A., “Quasi-Periodic Orbits About the Trans-Lunar Libration Point,” *Celestial Mechanics*, Vol. 7, No. 4, 1973, pp. 458–473. doi:10.1007/BF01227511
- [11] Farquhar, R., “The Utilization of Halo Orbits in Advanced Lunar Operations,” NASA, TN D-6365, 1971.
- [12] Breakwell, J., and Brown, J., “The ‘Halo’ Family of 3-Dimensional Periodic Orbits in the Earth–Moon Restricted 3-Body Problem,” *Celestial Mechanics*, Vol. 20, No. 4, 1979, pp. 389–404. doi:10.1007/BF01230405
- [13] Richardson, D. L., “Halo Orbit Formulation for the ISEE-3 Mission,” *Journal of Guidance and Control*, Vol. 3, No. 6, 1980, pp. 543–548. doi:10.2514/3.56033
- [14] Howell, K., “Three-Dimensional, Periodic, ‘Halo’ Orbits,” *Celestial Mechanics*, Vol. 32, No. 1, 1984, pp. 53–71. doi:10.1007/BF01358403
- [15] Howell, K., and Marchand, B., “Natural and Non-Natural Spacecraft Formations Near  $L_1$  and  $L_2$  Libration Points in the Sun-Earth/Moon Ephemeris System,” *Dynamical Systems: An International Journal*, Vol. 20, No. 1, March 2005, pp. 149–173.
- [16] McInnes, C., “Solar Sail Trajectories at the Lunar  $L_2$  Lagrange Point,” *Journal of Spacecraft and Rockets*, Vol. 30, No. 6, 1993, pp. 782–784. doi:10.2514/3.26393
- [17] Ozimek, M., Grebow, D., and Howell, K., “Solar Sails and Lunar South Pole Coverage,” AIAA Paper 2008-7080, Aug. 2008.
- [18] Baoyin, H., and McInnes, C., “Solar Sail Halo Orbits at the Sun-Earth Artificial  $L_1$  Point,” *Celestial Mechanics and Dynamical Astronomy*, Vol. 94, No. 2, 2006, pp. 155–171. doi:10.1007/s10569-005-4626-3
- [19] Baoyin, H., and McInnes, C., “Solar Sail Eequilibria in the Elliptical Restricted Three-Body Problem,” *Journal of Guidance, Control, and Dynamics*, Vol. 29, No. 3, 2006, pp. 538–543. doi:10.2514/1.15596
- [20] Baoyin, H., and McInnes, C., “Solar Sail Orbits at Artificial Sun-Earth Lagrange Points,” *Journal of Guidance, Control, and Dynamics*, Vol. 28, No. 6, 2005, pp. 1328–1331. doi:10.2514/1.14598
- [21] McInnes, C. R., “Artificial Lagrange Points for a Non-Perfect Solar Sail,” *Journal of Guidance, Control, and Dynamics*, Vol. 22, No. 1, 1999, pp. 185–187. doi:10.2514/2.7627
- [22] McInnes, C., McDonald, A., Simmons, J., and McDonald, E., “Solar Sail Parking in Restricted Three-Body Systems,” *Journal of Guidance, Control, and Dynamics*, Vol. 17, No. 2, 1994, pp. 399–406. doi:10.2514/3.21211
- [23] Simo, J., and McInnes, C. R., “Solar Sail Trajectories at the Earth–Moon Lagrange Points,” IAC Paper 08.C1.3.13, 29 Sept.–03 Oct. 2008.
- [24] Farquhar, R., “The Control and Use of Libration-Point Satellites,” Ph.D. Dissertation, Stanford University, 1968.